

# scientific data



OPEN

DATA DESCRIPTOR

## Multi-Planar Cervical Motion Dataset: IMU Measurements and Goniometer

Lee Keidan <sup>1,2,8</sup>, Rawan Ibrahim <sup>2,3,4,8</sup>, Evyatar Ohayon <sup>2</sup>, Chaim G. Pick <sup>1,2,5,6</sup> & Ella Been <sup>1,7</sup>✉

This data descriptor presents a comprehensive and replicable dataset and method for calculating the cervical range of motion (CROM) utilizing quaternion-based orientation analysis from Delsys inertial measurement unit (IMU) sensors. This study was conducted with 14 participants and analyzed 504 cervical movements in the Sagittal, Frontal and Horizontal planes. Validated against a Universal Goniometer and tested for reliability and reproducibility. Analysis showed strong validity in the sagittal plane ( $R = 0.828 \pm 0.051$ ) and moderate in the frontal ( $R = 0.573 \pm 0.138$ ), with limitations in the horizontal plane ( $R = 0.353 \pm 0.122$ ). Reliability was high across all planes (Sagittal:  $ICC = 0.855 \pm 0.065$ , Frontal:  $ICC = 0.855 \pm 0.015$ , Horizontal:  $ICC = 0.945 \pm 0.005$ ). Our model for CROM measurements is a valuable tool aiding diagnosis, treatment planning, and monitoring of cervical spine conditions. This study presents an accessible analysis process for biomechanical assessments in cervical and spinal fields. The dataset herein serves as a benchmark for state-of-the-art machine learning models predicting head/neck position, analyzing smoothness of movements, measuring standard motion patterns, and calibrating drift based on movement comparisons.

### Background & Summary

Cervical range of motion (CROM) biomechanical assessment is pivotal for objectively evaluating and analyzing human movement, identifying abnormalities, and guiding treatment progression. CROM is applicable in both clinical and experimental contexts, whether pre-operative, athletic performance, ergonomic evaluation, or pain management<sup>1</sup>. While other joints have enjoyed the limelight of past research, examining cervical motion remains a work in progress<sup>2-4</sup>.

The universal Goniometer (UG) has conventionally been favored by clinicians for CROM assessment due to its user-friendly nature, speed, and reasonable measurement of accuracy, thus deeming the UG the gold standard range of motion assessment tool, wildly used in clinical and academic settings<sup>5</sup>. Yet for CROM measurement, the UG has known limitations in accuracy and reproducibility, requiring trunk stabilization to measure pure CROM, limiting the examination to mostly upright positions, and leaving clinicians unable to measure neck CROM during different settings or more complex dynamic activities.

With the advancement of optical motion capture (mocap) systems, encompassing marker-based and marker-less technologies, a significant shift has emerged in the assessment of human motion. These systems especially when marker-based offer heightened accuracy, speed, and intuitive capability for capturing various angles across different planes and movements, frequently yielding reliable analyses of diverse body parts, including the upper limb. Consequently, marker-based mocap systems although very recent and still in the validation phase are starting to solidify as the gold standard in motion analysis. However, they are susceptible to some errors, particularly in joint position and near the axis of rotation<sup>6-8</sup>. Marker-based inaccuracies often arise from soft tissue artifacts, as muscle and skin move independently of the bone<sup>1,7-9</sup>. Additionally, optical motion capture

<sup>1</sup>Department of Anatomy and Anthropology, Faculty of Medical & Health Sciences, Tel-Aviv University, Tel-Aviv, 699780, Israel. <sup>2</sup>Sylvan Adams Sports Institute, Tel Aviv University, Tel Aviv, 699780, Israel. <sup>3</sup>Department of Biomedical Engineering, Faculty of Engineering, Tel-Aviv University, Tel-Aviv, 699780, Israel. <sup>4</sup>School of Electrical Engineering, Faculty of Engineering, Tel Aviv University, Tel Aviv, 699780, Israel. <sup>5</sup>The Dr. Miriam and Sheldon G. Adelson Chair and Center for the Biology of Addictive Diseases, Tel-Aviv University, Tel-Aviv, 699780, Israel. <sup>6</sup>Sagol School of Neuroscience, Tel Aviv University, Tel Aviv, 699780, Israel. <sup>7</sup>Department of Sports Therapy, Faculty of Health Professions, Ono Academic College, Kiryat Ono, 55000, Israel. <sup>8</sup>These authors contributed equally: Lee Keidan, Rawan Ibrahim. ✉e-mail: [beenella1@gmail.com](mailto:beenella1@gmail.com)

	Mean $\bar{x} \pm SD$ (Min-Max)
Age (y)	38 $\pm$ 13 (22–63)
Weight (Kg)	68 $\pm$ 12 (47–80)
Height (cm)	169 $\pm$ 8 (157–180)
Gender	6 Male, 8 Female

**Table 1.** Subject demographic data.

systems are also limited to specific laboratory-based settings, are highly expensive, and highly time-intensive, thus restricting their real-world applications<sup>9,10</sup>.

Over the past years, several studies have employed sensors to monitor physical parameters with a wide range of precision with regard to CROM measurements<sup>2,8,11,12</sup>. Furthermore, to be widespread in the clinical setting, these sensors must be user-friendly, comfortable, lightweight, and un-hindering to the wearer. The solution could rest with the Inertial Measurement Units (IMUs), an inexpensive, unrestricting way to measure these rotations<sup>2,13</sup>.

IMUs have been commercially available for some time and are utilized for various applications; however, more work needs to be done to determine the Reliability and Validity of these devices in different settings<sup>14</sup>, considering specific demands, including task, plane, and speed.

Although the assessment of movement utilizing IMU sensors has risen in the past ten years, the measurement of angular movements has proven problematic on numerous occasions, with papers either exhibiting discrepancies in Validity, a minimal number of participants, or unreplicable results<sup>13,15–21</sup>.

This study's aims to provide the foundational dataset and comprehensible workflow crucial for the development of many models, including machine learning (ML) models for predicting head/neck position in the space, analyzing smooth and healthy movements, measuring movement times in horizontal and vertical planes, and models for automatic calibration of sensor drift.

The initial goal is to serve as a foundational step in establishing clinical standards for dynamic CROM by providing a robust dataset and workflow. This dataset could enable the training of machine learning models to accurately predict head and neck positions based on IMU sensor, such models can be used in real-time applications to monitor and correct posture, potentially benefiting fields such as physical therapy, sports science, and ergonomics. In addition, the dataset provides detailed CROM data from healthy individuals, allowing for the analysis of smooth and natural cervical movements. This information can help establish normative data ranges and identify deviations in patients with movement disorders or injuries. Also, it captures movement times across different planes, reflecting normal cervical motion patterns at various speeds. This data could serve as a benchmark for understanding the dynamics of neck movements and can aid in designing rehabilitation protocols that mimic natural motion patterns. The dataset supports the development of models that can automatically calibrate drift by comparing the same movement in different body positions. Calibrating drift is essential for maintaining accuracy in long-term monitoring and ensuring consistent data quality across various conditions and environments. Automatic calibration will ensure reliability in long-term usage, which is critical in both clinical and real-world settings.

This dataset could serve as a foundation for future studies of all neck joints and test the sensor-to-segment calibration, essential for anatomically accurate joint angles in healthcare and rehabilitation. Sensor-to-segment calibration is a challenging notion as cervical measurements today, including the most popular UG assessment, cannot mimic anatomical cervical movement as the cervical angle is not made of one joint alone but derived from the combination of articulations produced between the occiput and the T1 vertebrae. Past research has attempted to carry out this work in the elbow joint successfully, yet much still needs to be done to achieve cervical sensor-to-segment calibration<sup>22,23</sup>.

This cervical movement data set encompasses 504 movements of all three cervical anatomical planes performed in horizontal and vertical positions. This study provides an accessible and comprehensible analysis process, allowing for an easily implemented and valuable accumulation of data for future works in the cervical or spinal field.

The cervical spine is one of the most complex systems in terms of articular motion. It includes seven cervical vertebrae and the skull, containing 37 separate joints that function simultaneously, allowing for small amounts of sliding and tilting between each joint. Due to this multi-joint structure, measuring the cervical spine's range of motion is highly complex and remains an ongoing challenge<sup>24,25</sup>. This study aims to adhere to the gold-standard assessment methodology of the Universal Goniometer (UG). In alignment with the UG, we evaluated the cervical angle by measuring inter-sensor angles rather than intersegmental or inter-joint calculations<sup>24,25</sup>.

## Methods

**Participants.** Fourteen asymptomatic participants (six males and eight females, age  $38 \pm 13$ ) were recruited for this study randomly from Tel-Aviv University staff via advertisements placed in the medical building and at Sylvan Adams Sports Institute. The inclusion criteria stated that participants had no history of neck injuries that required surgical intervention. The study was conducted at the Sylvan Adams Sports Institute at Tel Aviv University, Israel. Each participant signed an informed written consent waiver at the beginning of the study, providing approval for participation and data publication, under the Tel-Aviv University's ethics committee-approved study IRB 0007191-1. Any identifiable participant in this study has provided additional written consent for publication. Table 1 provides the demographic characteristics of subjects participating in the study.

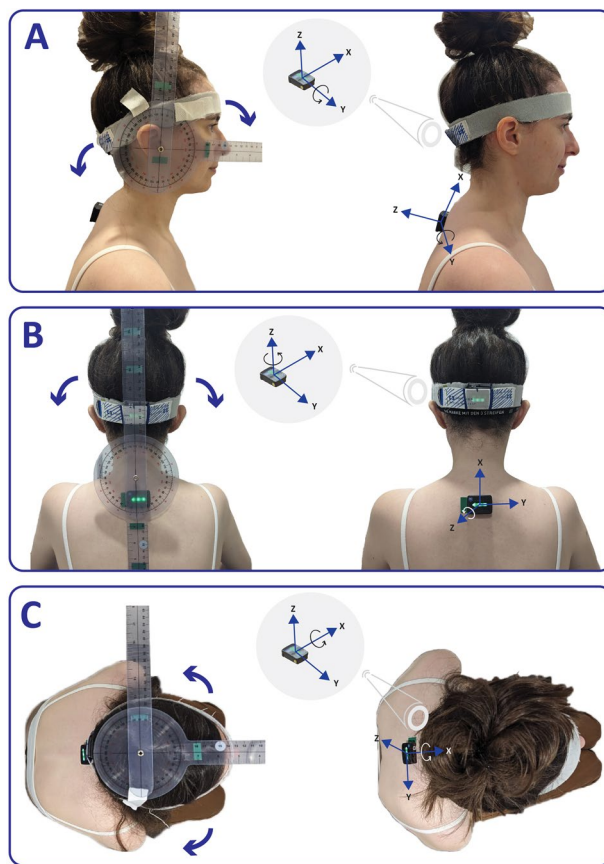


**Fig. 1** Universal goniometer, sensor placement, and reference system description. The Subject exhibits sensor and Goniometer placement for 3 planes. **(A)** Sagittal plane movement Flexion / Extension (Y axis). **(B)** Frontal plane movement, side Flexion (Z axis). **(C)** Horizontal plane movement, rotation (X-axis). The Individuals depicted have provided written consent for publication.

**Delsys trigno avanti sensors.** Two surface wireless 3D Delsys Trigno Avanti sensors (Delsys Inc, Natick, MA) embedded with EMG and IMU sensors, including a 3D accelerometer, 3D gyroscope, and 3D magnetometer, were used in this study. The choice of sensor was primarily due to the convenience of the future option of simultaneously extracting kinematic data and EMG acquisition in a single user-friendly program. Delsys provides a good platform for clinical work on both kinematic, EMG, and ECG acquisition from participants without the redundancy of multiple hardware and software.

The EMG sensor has an input range of 11 mV or 22 mV, a bandwidth of 10–850 Hz, and a resolution of 16 bits. The accelerometer offers a range of  $\pm 16$  g with a bandwidth of 24 Hz – 473 Hz and a resolution of 16 bits. The gyroscope features a range of  $\pm 2000$  dps, a bandwidth of 24 Hz – 360 Hz, and a resolution of 16 bits. The magnetometer has a range of  $\pm 4900$   $\mu$ T and a bandwidth of 50 Hz. Sampling rates for the sensors include an EMG sampling rate of 1259 Hz, an accelerometer, and a gyroscope sampling rate of 74 Hz. IMU orientation data was recorded using Delsys software EMGworks Acquisition 4.5.4 (Delsys Inc., Natick, MA, USA) with a sampling rate of 74 Hz. Data was received as quaternion elements using a built-in Delsys proprietary Kalman filter, where the magnetometer data is fused with the accelerometer and gyroscope data to estimate the orientation of the sensor in space.

**Data collection.** Sensors were used to monitor the participant's neck movements throughout the study. Sensor 1 was placed over the skin of the T1 vertebra with double-sided tape, and sensor 2 was placed inside a dedicated tightly fitted headband around the subject's head. The headband was then placed over the Occipital Protuberance and the Glabella. Sensor locations were based on recommendations made by past studies with minor modifications<sup>6</sup>, as shown in Fig. 1.

**Study measurements.** This data descriptor describes 84 healthy IMU measurements across 3 planes of cervical movements (Sagittal, Frontal, and Horizontal). In Part A, movements are produced vertically, and in Part B, they are produced again Horizontally. Another 84 UG measurements provide complementary Validity. This work analyzes and describes 504 IMU cervical movements (85X3X2).

**Experimental protocol.** *Part A (Validity).* The validation protocol was conducted with participants sitting upright (vertically) in a chair equipped with back support and armrests. Per the UG angle testing protocol,

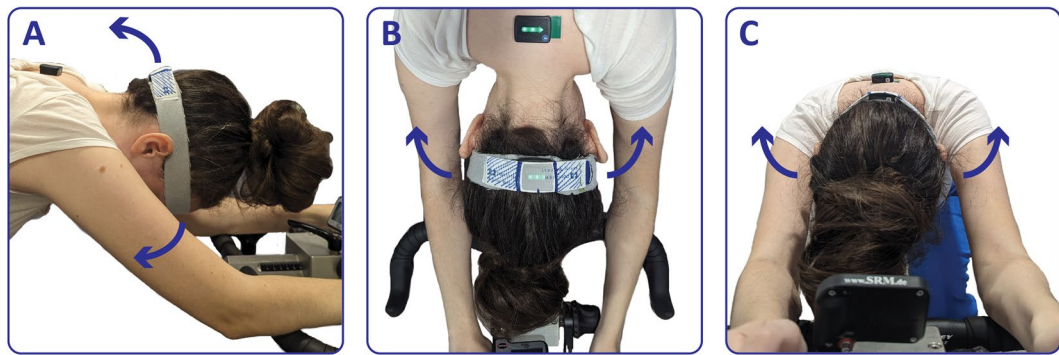


**Fig. 2** Sensor placement and body positioning for Part B. **(A)** Subject exhibiting flexion/extension (sagittal). **(B)** Subject exhibiting side flexion (Frontal). **(C)** Subject exhibiting rotation (Horizontal). The individuals depicted here have provided written consent for publication.

Participants were instructed to sit up straight, ensuring both feet were firmly and flat on the floor. Additionally, they were guided to position themselves as far back in the chair as possible while maintaining a neutral sitting position with thoracic and lumbar spine well supported by the chair back (baseline). Arms were to remain rested on the armrests throughout the protocol, as illustrated in Fig. 1<sup>24</sup>. The chair used in the study remained consistent throughout (40X40X45 cm) with consistent placement in the room. The electromagnetic field (EMF) was also tested prior to beginning the study, with minimal EMF determining the chair and SRM placement.

Aligning our sensors to the UG protocol bony surface anatomical landmarks (the spinous process of T1 and occipital bone) and adhering to this alignment throughout this study allowed for a methodical approach of sensor placement and minimal soft tissue artifact.

The protocol included movements on three anatomical planes recorded separately as trials:

- 1) **Trial 1:** Sagittal (Flexion/Extension).
- 2) **Trial 2:** Frontal (Left side flexion/ Right side flexion).
- 3) **Trial 3:** Horizontal (Rotation left/Rotation right).

The subjects were instructed to perform each movement to the full extent of their range of motion and then return to baseline. The protocol involved repeating each movement three times within a trial, resulting in six movements per trial.

Each trial began with 20 seconds devoted to calibration with the participant statically sitting, which provided the baseline measurement; the operator then aligned the UG. Goniometer active range of motion testing followed the protocol recommended by Norkin *et al.*<sup>17,24,26,27</sup>. A trained physical therapist experienced with the usage of the Universal Goniometer (LK) conducted the Goniometer measurement acquisition. (Fig. 1)

*Part B (Reliability).* This protocol included neck movement while leaning forward, as shown in Fig. 2. Subjects were instructed to maintain a horizontal state throughout this part of the study. In order to achieve this position, the subjects were statically seated on an SRM ergometer bike (Schöberer Rad-Messtechnik, SRM GmbH, Germany) with the handlebars dropped as they leaned forward on their forearms to perform the neck movements, thus achieving a horizontal state.

The protocol also included movements on three anatomical planes recorded separately as trials:

- 1) **Trial 4:** Sagittal (Flexion/Extension).
- 2) **Trial 5:** Frontal (Left side flexion/ Right side flexion).
- 3) **Trial 6:** Horizontal (Rotation left/Rotation right).

Participants performed three continuous movements during each trial, i.e., moving continuously from flexion to extension three times in succession. Subjects were instructed to perform each movement within a comfortable and repeatable range, remain in that range for 5 seconds for each movement, and then return to baseline. A retest protocol with the same exact methodology was initiated after a five-minute break.

The experimental workflow can be seen in Fig. 3.

The Validity of the UG device requires an upright vertical position to achieve textbook gold-standard use. Part B of this study does not include UG, so UG was not a hindering factor, allowing for the inclusion of both fluid motion and an addition of another plane in Part B. By Providing both vertical plane and horizontal plane testing options, the study made for a more well-rounded understanding of CROM in all planes.

**Data analysis.** MATLAB software (Mathworks Inc. Natick, MA, USA) was used for data analysis. Quaternion data of the Sagittal plane (Trial 1 and Trial 4) and Frontal plane (Trial 2 and Trial 5) were converted into absolute Euler angles ( $\theta_X$ ,  $\theta_Y$ ,  $\theta_Z$ ) for each sensor using MATLAB built-in function and wrapped to 360°, which uses the chosen segment (XYZ, ZYZ, ZYX) for calculated the Euler angles, the segments were chosen

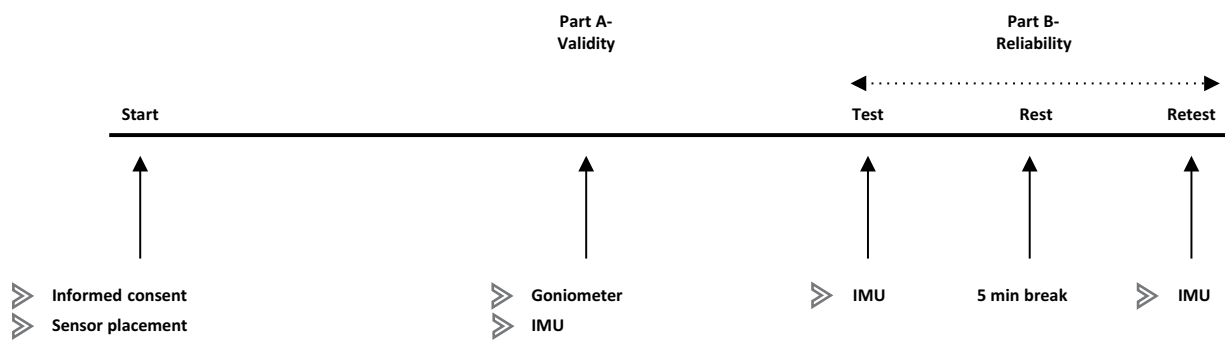


**Fig. 3** Experimental workflow.

manually for each trial and subject. The offset of the angles was calibrated manually according to the baseline to obtain the angle between the two sensors at the baseline position to be zero, as the offset in different planes and positions varied around zero depending on the subject's position and the chosen segment for the Euler angles calculations<sup>27–30</sup>.

The Euler angles between the sensors along the trial recording were calculated as the difference between them. The neck angle for Sagittal trials is  $\theta_Y$  of the difference, while for Frontal trials, it is  $\theta_Z$  of the difference.

Quaternion data of rotation (Trial 3 + 6) were converted into cartesian coordinates ( $S$ ) in 2D using the rotation matrix described in Eqs. (1–3) according to the chosen segment XYZ, ZYX, and ZYZ, respectively:

$$\text{Segment XYZ: } \begin{pmatrix} S_X \\ S_Y \end{pmatrix} = \begin{pmatrix} q_w^2 + q_x^2 - q_y^2 - q_z^2 \\ 2(q_x q_y + q_w q_z) \end{pmatrix} \quad (1)$$

$$\text{Segment ZYX: } \begin{pmatrix} S_X \\ S_Y \end{pmatrix} = \begin{pmatrix} 2(q_x q_y - q_w q_z) \\ 2(q_x q_z + q_w q_y) \end{pmatrix} \quad (2)$$

$$\text{Segment ZYZ: } \begin{pmatrix} S_X \\ S_Y \end{pmatrix} = \begin{pmatrix} 2(q_w q_y - q_x q_z) \\ 2(q_w q_z - q_x q_y) \end{pmatrix} \quad (3)$$

Where quaternion  $q$  is represented as:

$$q = q_w + q_x \hat{i} + q_y \hat{j} + q_z \hat{k}$$

The offset of the Cartesian coordinates for sensor 1 was adjusted relative to the baseline, setting it to (1,0). Similarly, the coordinates for sensor 2 were aligned with the baseline, set to (0,0). This adjustment facilitated the calculation of angles between the two vectors. The angle between the two vectors was calculated according to Equation 4, which represents the neck's angle:

$$\theta_{1-2} = \left( \frac{\underline{S1} \cdot \underline{S2}}{\|\underline{S1}\| \|\underline{S2}\|} \right) \quad (4)$$

where  $S1$  and  $S2$  are the cartesian coordinates of sensor 1 and sensor 2, respectively. Eventually, the angle of each movement extracted as the mean of ~0.5 sec of steady angle without any noise, or movement.

**Statistical analysis.** *Part A.* In order to assess the quality of measurements, IMU data was compared to gold standard noninvasive UG<sup>1,26</sup>, obtaining Validity. Results were analyzed via SPSS 27 and Python. Following the D'Agostino & Pearson test for normality, all but 1 of the parameters studied proved normally distributed. Thus, Validity was assessed using the Pearson correlation between the UG and IMU results. Additionally, modified Bland-Altman analyses (Fig. 5), incorporating random effects models for enhanced precision in estimating within-subject variance (WSV), were conducted to assess agreement between the two measurement methods with repeated measures as proposed by Myles *et al.*<sup>27</sup>.

Power analysis was conducted using G\*Power 3.1 (Faul *et al.*<sup>31,32</sup>). For correlation analysis of both test parts, with the minimum acceptable power level of 0.80 and  $N = 14$ , the minimum required correlation coefficient is 0.67. Correlation coefficients that are between 0.62 and 0.67 achieve an accepted level of power of 0.70 to 0.80. All coefficients that are below 0.62 demonstrate lower power<sup>31,32</sup>.

		Repetition 1	Repetition 2	Repetition 3	Mean $\bar{x} \pm SD$
Sagittal	Flexion	$r = 0.78$	$r = 0.78$	$r = 0.91$	$r = 0.82 \pm 0.075$
	Extension	$r = 0.88$	$r = 0.81$	$r = 0.81$	$r = 0.83 \pm 0.04$
Frontal	Side flexion left	$r = 0.68$	$r = 0.64$	$r = 0.41$	$r = 0.58 \pm 0.14$
	Side flexion right	$r = 0.7$	$r = 0.74$	$r = 0.37$	$r = 0.61 \pm 0.20$
Horizontal	Rotation left	$r = 0.30$	$r = 0.27$	$r = 0.18$	$r = 0.28 \pm 0.06$
	Rotation right	$r = 0.53$	$r = 0.50$	$r = 0.34$	$r = 0.46 \pm 0.10$

**Table 2.** Validity (Part A). Validity of cervical range of motion for each cervical movement in accordance with the description in *Part A*, *i.e.*, both Flexion/Extension (Sagittal/Pitch), Side flexion Left/ Side flexion Right (Frontal/Roll) and Rotation Left/Rotation Right (Horizontal/Yaw). Table indicates the Pearson  $r$  score for the Range of motion between the Universal Goniometer and the wearable internal measurement sensor for each cervical movement. Validation is provided both divided by repetition and for all repetitions.

	Repetition 1		Repetition 2		Repetition 3		All	
	Pre	Post	Pre	Post	Pre	Post	Pre	Post
	$32.4 \pm 16.6$	$36.3 \pm 15.4$	$33.1 \pm 16.5$	$35.3 \pm 16.4$	$33.3 \pm 16.8$	$35.1 \pm 16.7$	$32.9 \pm 16.8$	$35.6 \pm 16.2$
Flexion (°)	ICC = 0.89		ICC = 0.95		ICC = 0.91		ICC = 0.92 $\pm 0.02$	
	$47.1 \pm 24.9$	$43.7 \pm 22.3$	$47.2 \pm 24.5$	$43.8 \pm 19.5$	$48.1 \pm 24.8$	$43.6 \pm 19.5$	$47.5 \pm 24.7$	$43.7 \pm 20.4$
Extension (°)	ICC = 0.83		ICC = 0.79		ICC = 0.76		ICC = 0.79 $\pm 0.03$	
	$49 \pm 19$	$50 \pm 13$	$51 \pm 14$	$51 \pm 15$	$51 \pm 12$	$50 \pm 11$	$50 \pm 15$	$50 \pm 13$
Side flexion left (°)	ICC = 0.85		ICC = 0.83		ICC = 0.83		ICC = 0.84 $\pm 0.01$	
	$57 \pm 25$	$54 \pm 23$	$54 \pm 23$	$54 \pm 22$	$52 \pm 24$	$55 \pm 21$	$54 \pm 24$	$55 \pm 22$
Side flexion right (°)	ICC = 0.94		ICC = 0.92		ICC = 0.75		ICC = 0.87 $\pm 0.1$	
	$63.7 \pm 12$	$62.7 \pm 15.2$	$63.8 \pm 15$	$64.3 \pm 14.6$	$63.8 \pm 15.2$	$63.2 \pm 14.8$	$63.8 \pm 14.1$	$63.4 \pm 14.9$
Rotation left (°)	ICC = 0.92		ICC = 0.96		ICC = 0.95		ICC = 0.94 $\pm 0.02$	
	$66.5 \pm 15$	$65 \pm 14.8$	$65.5 \pm 16.5$	$65.1 \pm 16$	$65.6 \pm 17.4$	$66 \pm 16.6$	$65.9 \pm 16.3$	$65.4 \pm 15.8$
Rotation right (°)	ICC = 0.94		ICC = 0.94		ICC = 0.96		ICC = 0.95 $\pm 0.01$	

**Table 3.** Reliability (Part B). Interclass Correlation Coefficient scores (ICC) and individual mean and SD scores for each pair of test-retest sensor measurements related to each cervical movement. Data is divided by repetition.

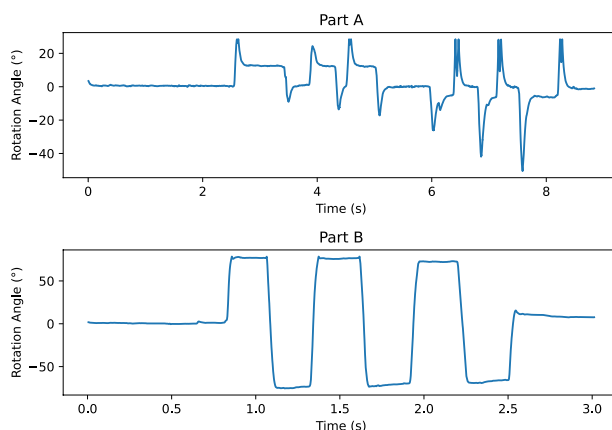


**Fig. 4** The subject performed cervical rotation in both experimental parts of the testing. Part A -The subject performed six rotations, rotations to the Left (negative), exhibiting angles with no steady state. Part B- exhibiting smooth right (positive) and left (negative) Rotation.

The sample size was not affected by the typical approach focusing on an extensive number of subjects at the cost of accurate human movement. The priority here was providing a data set that accurately characterizes and records cervical movement and tracking neck angles<sup>21</sup>. We expect that this dataset will provide a base for statistical comparisons between clinical groups or for machine learning identifying cervical movement patterns; thus, we decided to focus on attaining high-quality cervical movement patterns in all anatomical plains, both vertically and horizontally, with a large amount of data per subject rather than a large number of subjects. Still, this approach does not compromise the Power analysis and aligns with past studies conducted in the same field<sup>33</sup>.

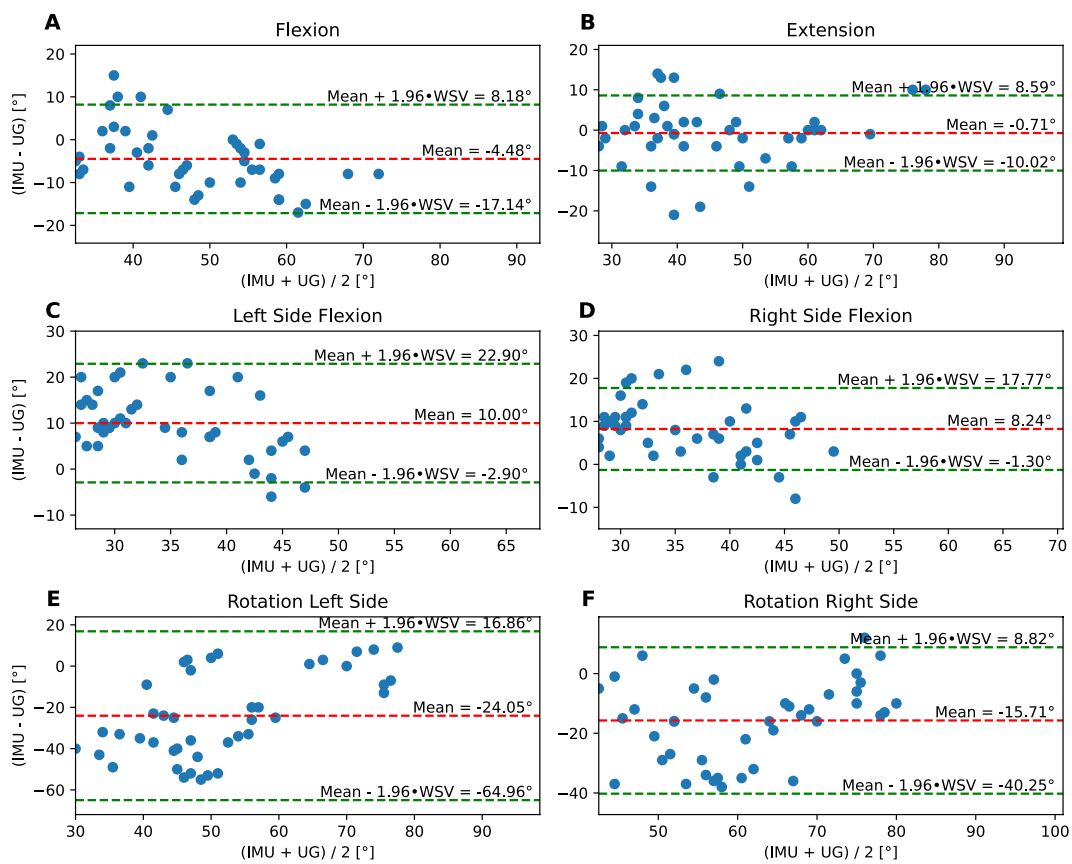


**Fig. 5** Bland-Altman plots. Comparison of IMU sensor to Goniometer Range of Motion for (A) Flexion, (B) Extension, (C) Side flexion left, (D) Side flexion right, (E) Rotation left, (F) Rotation right. The mean difference is displayed as a dashed red line, while the upper and lower modified limits of agreement are displayed as dashed green lines.

*Part B.* The test-retest protocol was administered to estimate relative Reliability. Relative Reliability was assessed using inter-class correlation (ICC- Two-way random effect, absolute agreement, single rater).

Pearson and ICC effect values were interpreted following the Davis' (1971) Guidelines for the Interpretation of Effect Size for Correlations; as such,  $r > 0.7$  was regarded as a very strong association,  $0.69 < r > 0.5$  substantial level  $0.49 < r > 0.3$  moderate  $0.29 < r > 0.1$  low  $r < 0.1$  negligible.

## Data Records

The data record for each of the fourteen subjects is stored in the figshare repository as .csv files<sup>34</sup>. The dataset consists of a folder of csv files stored in the Dataset directory for each subject. Each csv file contains the recording session of a subject named after the experiment part and anatomical plane, with multiple columns representing the measurements taken during the experiment. File name is {date of experiment}\_{subject code}\_{experimental part: A or B}\_{anatomical plane tested: Frontal or Sagittal or Horizontal}\_{for part B: Pre-test or Post-test}.csv.

Each file contains columns representing various measurements taken during the experiment, including quaternion coordinates over time for the two sensors.

## Technical Validation

Sagittal plane (Flexion/Extension) and Frontal plane (Side flexion Left/Right)-Pearson correlation score three repetitions IMU sensors demonstrated a very strong level of Validity compared to the gold standard UG, (Table 2). Figure 4 is within an acceptable range.

The Horizontal plane (Left/Right Rotation) was relatively low. The limits of agreement are relatively high. Table 2, Figure 4.

Reliability of IMUs in Cervical Range of Motion Assessment: Intraclass correlation coefficients (ICC) were calculated to assess the Reliability for Flexion/Extension, Left/Right Side flexion, and Left/Right Rotation for all three repetitions (Part B). The ICC results, as shown in Table 3, conclude that each subject's IMU measurements are consistent over time. These high ICC values indicate excellent Reliability for IMU in measuring the cervical range of motion across various planes. The results suggest that IMU are a highly suitable device for repeated measurements.

Table 4 shows the Reliability of UG measurements, comparing our results to past studies regarding normative CROM.

	Universal Goniometer	IMU		Wilson-Smith Univers 1 Goniometer (mean age = 20, n = 50)	Wolan-Nieroda CROM Device (mean age = 21, n = 95)	Khan Universal Goniometer (mean age = 32, n = 60)	Youdas Universal Goniometer (mean age = 59, n = 20)	Tousignant CROM Device (mean age = 51, n = 55)
	Vertical	Vertical position	Horizontal position					
Flexion (°)	50 ± 12	46 ± 9	32.92 ± 16.8	38.3 ± 8.9	55.7 ± 8.05	44.6 ± 1.3	40 ± 12	47 ± 11
Extension (°)	44 ± 14	44.073 ± 14	47.47 ± 24.7	59.6 ± 15.0	88.33 ± 15.75	43.4 ± 1.6	50 ± 14	50 ± 14
Side flexion left (°)	30 ± 9	36 ± 7	50 ± 15	31.3 ± 7.0	47.7 ± 9.75	43.1 ± 2.4	22 ± 7	33 ± 9
Side flexion right (°)	31 ± 8	40 ± 9	54 ± 24	35.2 ± 6.4	45.2 ± 8.9	43.7 ± 2.1	22 ± 8	30 ± 9
Rotation left (°)	64 ± 11	40 ± 21	64 ± 14	61.0 ± 13.3	61.73 ± 13.9	79.2 ± 2.2	51 ± 11	56 ± 12
Rotation right (°)	69 ± 11	54 ± 15	66 ± 16	63.0 ± 11.6	72.67 ± 9.8	79.1 ± 2.2	49 ± 9	56 ± 10

**Table 4.** Mean and SD, Range of Motion analysis for each cervical movement compared to past studies conducted using the Universal Goniometer or a similar device.

## Limitations

We acknowledge that the choice to conduct this research using the Delsys Trigno Avanti sensors, although based on the previous knowledge that these sensors are both widely used in different clinical and research settings, are portable, easy to use, record, and store the data could have yielded varied results from other known IMU sensors<sup>35</sup>.

Calibration and specifically magnetometer alignment between sensors, while carefully conducted, introduces a potential for error that could have influenced our data collection, especially rotation conducted in the Yaw axis. The methodology of processing quaternion data and angle calculation, although suitable in the context of this study, could have limitations for other approaches. Moreover, we acknowledge that the recurring spiked end CROM on the left side with no apparent steady state as the subjects persisted in staying at end CROM (during UG examination part A as seen in Fig. 2) is still a concern and provides an additional limitation.

The clinical setting may encounter external factors we have yet to foresee, which could still harbor additional hindering problems.

## Usage Notes

Following the processing workflow in our code will help mitigate limitations as much as possible.

## Code availability

The study's code is fully available in git ([https://github.com/RawanIb/Multi-Planar\\_Cervical\\_Motion\\_Dataset\\_IMU\\_Measurements\\_and\\_Goniometer.git](https://github.com/RawanIb/Multi-Planar_Cervical_Motion_Dataset_IMU_Measurements_and_Goniometer.git)).

Received: 22 March 2024; Accepted: 20 December 2024;

Published online: 03 January 2025

## References

1. Haimovich, Y., Hershkovich, O., Portnoy, S., Schwartz, I. & Lotan, R. Evaluating Lower Limb Kinematics Using Microsoft's Kinect: A Simple, Novel Method. *Physiother Can* **73**, 391–400 (2021).
2. Rigoni *et al.* Assessment of Shoulder Range of Motion Using a Wireless Inertial Motion Capture Device—A Validation Study. *Sensors* **19**, 1781 (2019).
3. Camargo, J., Ramanathan, A., Flanagan, W. & Young, A. A comprehensive, open-source dataset of lower limb biomechanics in multiple conditions of stairs, ramps, and level-ground ambulation and transitions. *J Biomech* **119**, 110320 (2021).
4. Scherpereel, K., Molinaro, D., Inan, O., Shepherd, M. & Young, A. A human lower-limb biomechanics and wearable sensors dataset during cyclic and non-cyclic activities. *Sci Data* **10**, 924 (2023).
5. Wilson-Smith, A. R. *et al.* Validation of a novel range of motion assessment tool for the cervical spine: the HALO© digital goniometer. *Journal of Spine Surgery* **8**, 93–102 (2022).
6. Dahl, K. D., Dunford, K. M., Wilson, S. A., Turnbull, T. L. & Tashman, S. Wearable sensor validation of sports-related movements for the lower extremity and trunk. *Med Eng Phys* **84**, 144–150 (2020).
7. Mchugh, B., Akhbari, B., Morton, A. M., Moore, D. C. & Crisco, J. J. Optical motion capture accuracy is task-dependent in assessing wrist motion. *J Biomech* **120** (2021).
8. Kuster, R. P., Heinlein, B., Bauer, C. M. & Graf, E. S. Accuracy of KinectOne to quantify kinematics of the upper body. *Gait Posture* **47**, 80–85 (2016).
9. Miranda, D. L., Rainbow, M. J., Crisco, J. J. & Fleming, B. C. Kinematic differences between optical motion capture and biplanar videoradiography during a jump-cut maneuver. *J Biomech* **46**, 567–573 (2013).
10. Wade, L., Needham, L., McGuigan, P. & Bilzon, J. Applications and limitations of current markerless motion capture methods for clinical gait biomechanics. *PeerJ* **10**, e12995 (2022).
11. Martínez-Hernández, A., Pérez-Lomelí, J. S., Burgos-Vargas, R. & Padilla-Castañeda, M. A. A Wearable System Based on Multiple Magnetic and Inertial Measurement Units for Spine Mobility Assessment: A Reliability Study for the Evaluation of Ankylosing Spondylitis. *Sensors* **22**, 1332 (2022).
12. Maselli, M. *et al.* A Wearable Sensing Device for Monitoring Single Planes Neck Movements: Assessment of Its Performance. *IEEE Sens J* **18**, 6327–6336 (2018).
13. Tolza, X., Soto-Romero, G., Fourniols, J. Y. & Acco, P. Preliminary study: IMU system validation for real-time feedback on swimming technique. *Comput Methods Biomed Engin* **20**, S203–S204 (2017).
14. Taylor, L., Miller, E. & Kaufman, K. R. Static and dynamic validation of inertial measurement units. *Gait Posture* **57**, 80–84 (2017).
15. Morrow, M. M. B., Lowndes, B., Fortune, E., Kaufman, K. R. & Hallbeck, M. S. Validation of Inertial Measurement Units for Upper Body Kinematics. *J Appl Biomech* **33**, 227–232 (2017).
16. Chan, L. Y. T. *et al.* Assessment of shoulder range of motion using a commercially available wearable sensor—a validation study. *Mhealth* **8**, 30–30 (2022).

17. Yoon, T.-L., Kim, H.-N. & Min, J.-H. Validity and Reliability of an Inertial Measurement Unit-based 3-Dimensional Angular Measurement of Cervical Range of Motion. *J Manipulative Physiol Ther* **42**, 75–81 (2019).
18. Seong, M. *et al.* MultiSenseBadminton: Wearable Sensor-Based Biomechanical Dataset for Evaluation of Badminton Performance. *Sci Data* **11**, 343 (2024).
19. Wong, C., Zhang, Z., Lo, B. P. L. & Yang, G.-Z. Wearable Sensing for Solid Biomechanics. *IEEE Sens J* **1**–1, <https://doi.org/10.1109/JSEN.2015.2393883> (2015).
20. Rekant, J., Rothenberger, S. & Chambers, A. Inertial measurement unit-based motion capture to replace camera-based systems for assessing gait in healthy young adults: Proceed with caution. *Measurement: Sensors* **23**, 100396 (2022).
21. Wiles, T. M. *et al.* NONAN GaitPrint: An IMU gait database of healthy young adults. *Sci Data* **10**, 867 (2023).
22. Bonfiglio, A., Tacconi, D., Bongers, R. M. & Farella, E. Effects of IMU sensor-to-segment calibration on clinical 3D elbow joint angles estimation. *Front Bioeng Biotechnol* **12** (2024).
23. Choe, N., Zhao, H., Qiu, S. & So, Y. A sensor-to-segment calibration method for motion capture system based on low cost MIMU. *Measurement* **131**, 490–500 (2019).
24. Norkin, C. C., and D. J. W. *Measurement of Joint Motion: A Guide to Goniometry*. (FA Davis, 2016).
25. Bland, J. H. & Boushey, D. R. Anatomy and physiology of the cervical spine. *Semin Arthritis Rheum* **20**, 1–20 (1990).
26. Franco, L., Sengupta, R., Wade, L. & Cazzola, D. A novel IMU-based clinical assessment protocol for Axial Spondyloarthritis: a protocol validation study. *PeerJ* **9**, e10623 (2021).
27. Myles, P. S. & Cui, J. I. Using the Bland–Altman method to measure agreement with repeated measures. *Br J Anaesth* **99**, 309–311 (2007).
28. Kaufman-Cohen, Y. *et al.* Wrist Plane of Motion and Range During Daily Activities. *The American Journal of Occupational Therapy* **72**, 7206205080p1–7206205080p10 (2018).
29. Henschke, J., Kaplick, H., Wochatz, M. & Engel, T. Assessing the validity of inertial measurement units for shoulder kinematics using a commercial sensor-software system: A validation study. *Health Sci Rep* **5** (2022).
30. Lee, R., Akhundov, R., James, C., Edwards, S. & Snodgrass, S. J. Variations in Concurrent Validity of Two Independent Inertial Measurement Units Compared to Gold Standard for Upper Body Posture during Computerised Device Use. *Sensors* **23**, 6761 (2023).
31. Faul, F., Erdfelder, E., Buchner, A. & Lang, A.-G. Statistical power analyses using G\*Power 3.1: Tests for correlation and regression analyses. *Behav Res Methods* **41**, 1149–1160 (2009).
32. Faul, F., Erdfelder, E., Lang, A.-G. & Buchner, A. G\*Power 3: A flexible statistical power analysis program for the social, behavioral, and biomedical sciences. *Behav Res Methods* **39**, 175–191 (2007).
33. AlDahas, A., Devecchi, V., Deane, J. A. & Falla, D. Measurement properties of cervical joint position error in people with and without chronic neck pain. *PLoS One* **18**, e0292798 (2023).
34. Keidan, L., Ibrahim, R., Ohayon, E., Pick, C. G. & Been, E. Multi-Planar Cervical Motion Dataset: IMU Measurements and Goniometer. *figshare* <https://doi.org/10.6084/m9.figshare.26935900> (2024).
35. Manupibul, U. *et al.* Integration of force and IMU sensors for developing low-cost portable gait measurement system in lower extremities. *Sci Rep* **13**, 10653 (2023).

## Acknowledgements

The authors thank the participants in this study especially those who approved the publication of identifiable footage.

## Author contributions

L.K. - collected the data; conceived and designed the analysis; performed the analysis and the interpretation of the results; wrote the manuscript. R.I. - conceived and designed the analysis; performed the analysis and the interpretation of the results; wrote the manuscript. E.O. - performed the analysis and the interpretation of the results. C.G.P. – study conception and design; study supervision; results interpretation; reviewed and edited the manuscript. E.B. – study conception and design; study supervision; results interpretation; reviewed and edited the manuscript. All authors read and approved the final manuscript.

## Competing interests

The authors declare no competing interests.

## Additional information

**Correspondence** and requests for materials should be addressed to E.B.

**Reprints and permissions information** is available at [www.nature.com/reprints](http://www.nature.com/reprints).

**Publisher's note** Springer Nature remains neutral with regard to jurisdictional claims in published maps and institutional affiliations.



**Open Access** This article is licensed under a Creative Commons Attribution-NonCommercial-NoDerivatives 4.0 International License, which permits any non-commercial use, sharing, distribution and reproduction in any medium or format, as long as you give appropriate credit to the original author(s) and the source, provide a link to the Creative Commons licence, and indicate if you modified the licensed material. You do not have permission under this licence to share adapted material derived from this article or parts of it. The images or other third party material in this article are included in the article's Creative Commons licence, unless indicated otherwise in a credit line to the material. If material is not included in the article's Creative Commons licence and your intended use is not permitted by statutory regulation or exceeds the permitted use, you will need to obtain permission directly from the copyright holder. To view a copy of this licence, visit <http://creativecommons.org/licenses/by-nc-nd/4.0/>.

© The Author(s) 2025